Electronic Supplementary Information

Rapid Glycoconjugation with Glycosyl Amines

Mareike A. Rapp,[a] Oliver R. Baudendistel,[a] Ulrich E. Steiner [a] and Valentin Wittmann *[a]

[a] *Department of Chemistry and Konstanz Research School Chemical Biology (KoRS-CB), University of Konstanz, Universitätsstraße 10, 78457 Konstanz, Germany. E-mail: mail@valentin-wittmann.de*

Table of Content

Experimental Procedures

Synthesis of $GlcNAcNH_2$ (10)

$GlcNAcNH_2$ (**10**) was obtained by hydrogenation of $GlcNAcN_3$ (**9**)[1] (19.4 mg, 0.08 mmol) with Pd/C (5% on carbon, wetted with ca. 55% water, 9.4 mg) in dry MeOH (2.0 mL). The mixture was stirred under a hydrogen atmosphere until TLC indicated complete conversion and was then immediately filtered through a short plug of celite or a syringe filter. The solvent was removed and the residual glycosyl amine was used without further purification. $GlcNAcNH_2$ was obtained as colorless solid (17.6 mg, quant.). Spectroscopic data were in accordance with literature.[2]

Deuterated buffer containing 2 mM trimethylsilylpropanoic acid (TSP)

To prepare 10 mL buffer, the required ingredients (TSP, ammonium acetate-d_7 or KD_2PO_4) were dissolved in D_2O (8 mL). Subsequently, the pH was adjusted with CD_3CO_2D or NaOD in D_2O to the desired value and the solution diluted to a final volume of 10 mL with D_2O. To determine the pH, a pH-meter that had been calibrated in non-deuterated buffers, was employed. The value pH* displayed by the instrument, was converted to the real pH according to the formula pH = 0.9291 × pH*+ 0.421.[3]

Oxyamine stock solution

Stock solutions of ethoxyamine (bought as the HCl salt), were prepared in deuterated acetate or phosphate buffer (250 or 500 mM, 2 mM TSP). After dissolution, the pH was readjusted to the desired value with CD_3CO_2D or NaOD in D_2O.

NMR monitoring of $GlcNAcNH_2$ hydrolysis and reaction of oxyamine with $GlcNAcNH_2$ or GlcNAc

$GlcNAcNH_2$ (**10**) was freshly prepared for each experiment and its integrity checked by ^{1}H NMR. The carbohydrate was dissolved in buffer (hydrolysis experiments) or an oxyamine stock solution (ligation experiments) to the final concentrations given below. The reaction mixture was transferred into a 5 mm NMR tube and the reaction was immediately followed by ^{1}H NMR spectroscopy. Spectra were recorded with 4 scans (using a *Bruker* Avance III 600 MHz instrument) or 1 scan (using a *Bruker* Avance NEO 800 MHz instrument) and a pulse angle of 30°. A relaxation delay of 20 s was used. For integration of ^{1}H spectra, only well-separated resonances were used. Multiple point baseline correction was performed to ensure baseline separated peaks. The integrals were converted to concentrations using the known concentration of added standard (TSP). ^{1}H chemical shifts are referenced to the TSP signal (δ_H = 0.00 ppm). The combined yields of all forming products ((*E*)- and (*Z*)-oximes and *N*-glycosyl oxyamine) (ligation experiments) or remaining $GlcNAcNH_2$ (hydrolysis experiments) was plotted over time using Origin 9.8.0.200. A logarithmic x-axis was chosen for a better resolution of the high reaction speed at the beginning of the reaction. Due to the release of NH_3 during consumption of $GlcNAcNH_2$ the stability of the buffered system, thus steadiness of pH was ensured by checking the pH after the experiments.

Hydrolysis experiments

pH 5–7: 5 mM sugar, 200-500 mM ammonium acetate-d_7 buffer, 39 °C

pH 8: 10 mM sugar, 250 mM KD_2PO_4 buffer, 39 °C

Oxyamine ligation experiments

pH 5–7: 36 mM sugar, 5 equiv. ethoxyamine, 500 mM ammonium acetate-d_7 buffer, 39 °C

pH 5–7: 5 mM sugar, 10 equiv. ethoxyamine, 250 mM ammonium acetate-d_7 buffer, 39 °C

pH 6: 5 mM sugar, 20 and 50 equiv. ethoxyamine, 250 mM ammonium acetate-d_7 buffer, 39 °C

pH 8: 36 mM sugar, 5 equiv. ethoxyamine, 500 mM KD_2PO_4 buffer, 39 °C

pH 8: 5 mM sugar, 10 equiv. ethoxyamine, 250 mM KD_2PO_4 buffer, 39 °C

Deglycosylation of RNase B with PNGase F and ligation to oxyamine linker 13

A stock solution (10 mg mL^{-1}) of RNase B (*Abnova*) in ultrapure water (225 µL) was diluted with 15 µL ultrapure water and 60 µL of 5x Rapid PNGase F buffer (*New England Biolabs*) to a final volume of 300 µL. To denature the protein, the sample was incubated at 80 °C for 2 min and then cooled down. 15 µL Rapid PNGase F (*New England Biolabs*) was added to the sample and the mixture was incubated at 50 °C for 10 min according to the Rapid PNGase F kit manual provided by manufacturer. The reaction mixture was lyophilized and then incubated with a 75 mM solution of oxyamine linker **13**[4] in ammonium acetate buffer (250 mM, 20 µL) at pH 6.

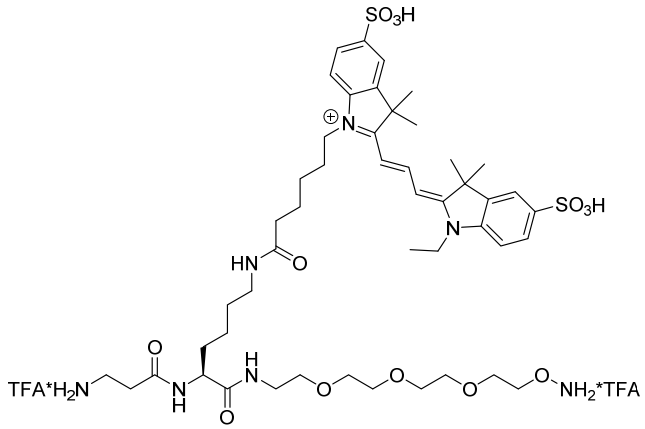

13

After 4 h the reaction mixture was diluted with ammonium acetate buffer pH 6 (250 mM, 90 µL) and high-loading TentaGel resin with aldehyde groups (TentaGel® HL CHO Resin, 0.4–0.6 mmol g^{-1}, *Rapp Polymere*) (16 mg) was added to the reaction tube. The mixture was shaken at RT and the resin removed by using a SigmpaPrep spin column (*Sigma-Aldrich*) and a tabletop centrifuge (1 min, 10000 rpm). Subsequently, the filtrate was purified over an Amicon Ultra 0.5 mL centrifugal filter with a 10 kDa cutoff (*Merck*) and lyophilized. Prior to purification, the Amicon device was washed with 0.1 M NaOH (1 x 200 µL) and ultrapure water (2 x 400 µL) at 14000 x g for 5 min each.

LC-MS/MS analysis of released glycans conjugated to linker 13

The released glycans conjugated to linker **13** were analyzed by reversed-phase liquid chromatography nanospray tandem mass spectrometry (LC-MS/MS) using an LTQ-Orbitrap mass spectrometer (*Thermo Fisher Scientific*) and an Eksigent nano-HPLC. Used reversed-phase LC column: 5 µm, 100 Å pore size C18 resin, 75 µm i.d. × 15 cm, fused silica capillary (Acclaim PepMap100, *Thermo Fisher Scientific*). After sample injection, the column was washed for 5 min with 90% mobile phase A (0.1% aqueous formic acid) and 10% mobile phase B (0.1% formic acid in acetonitrile) and peptides were eluted using a linear gradient of 10% mobile phase B to 35% mobile phase B in 25 min, then to 100% B in an additional 1 min, at 300 nL/min. The LTQ-Orbitrap mass spectrometer was operated in a data-dependent mode in which each full MS scan (30 000 resolving power) was followed by ten MS/MS scans where the ten most abundant molecular ions were dynamically selected and fragmented by collision-induced dissociation (CID) using a normalized collision energy of 35% in the LTQ ion trap. Dynamic exclusion was allowed.

Supplementary Figures

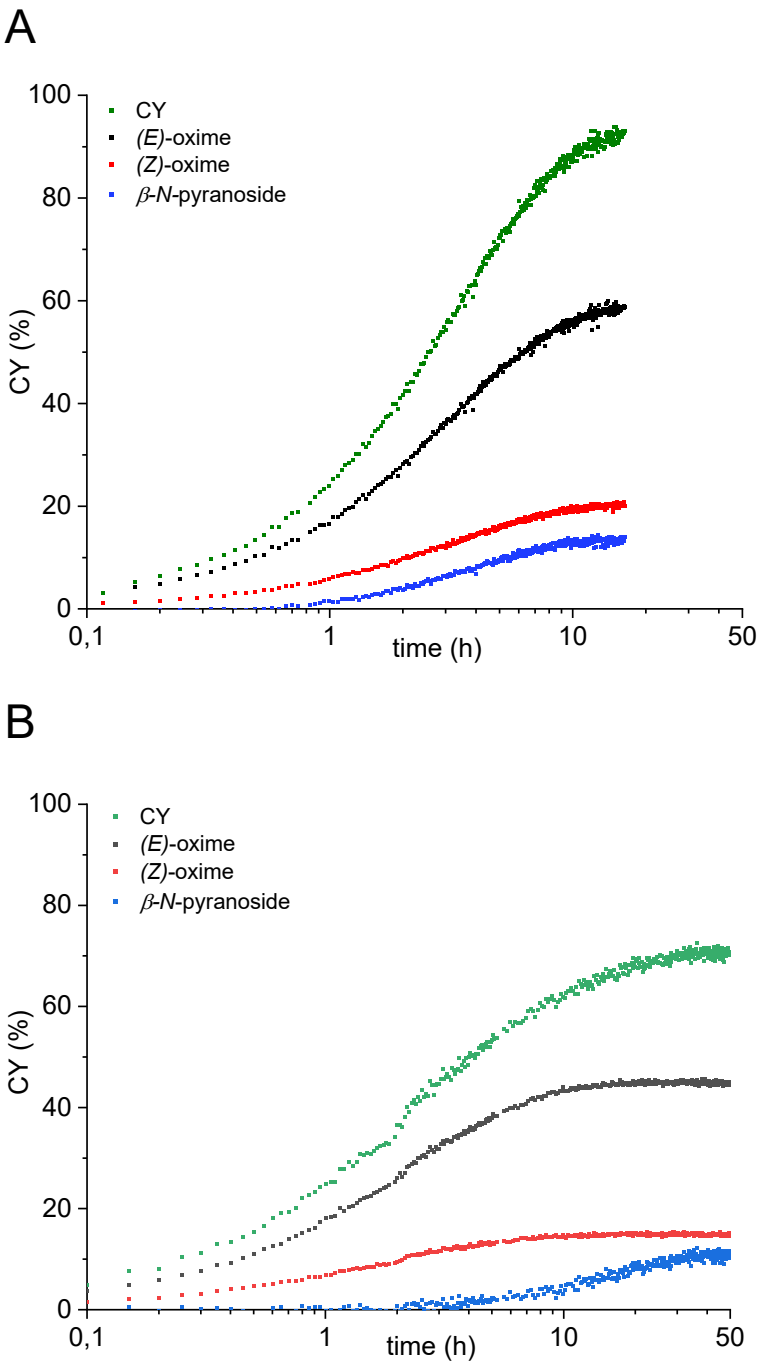

Figure S1. Individual yields of ligation products ((*E*)- and (*Z*)-oximes **11** and *N*-glycosyl oxyamine **12**) and combined yield CY of the oxyamine ligation reaction of (A) GlcNAc (36 mM) and ethoxyamine (180 mM) in 500 mM ammonium acetate-d_7 buffer at 39 °C and pH 5 and (B) $GlcNAcNH_2$ **10** (36 mM) and ethoxyamine (180 mM) in 500 mM KD_2PO_4 buffer at 39 °C and pH 8.

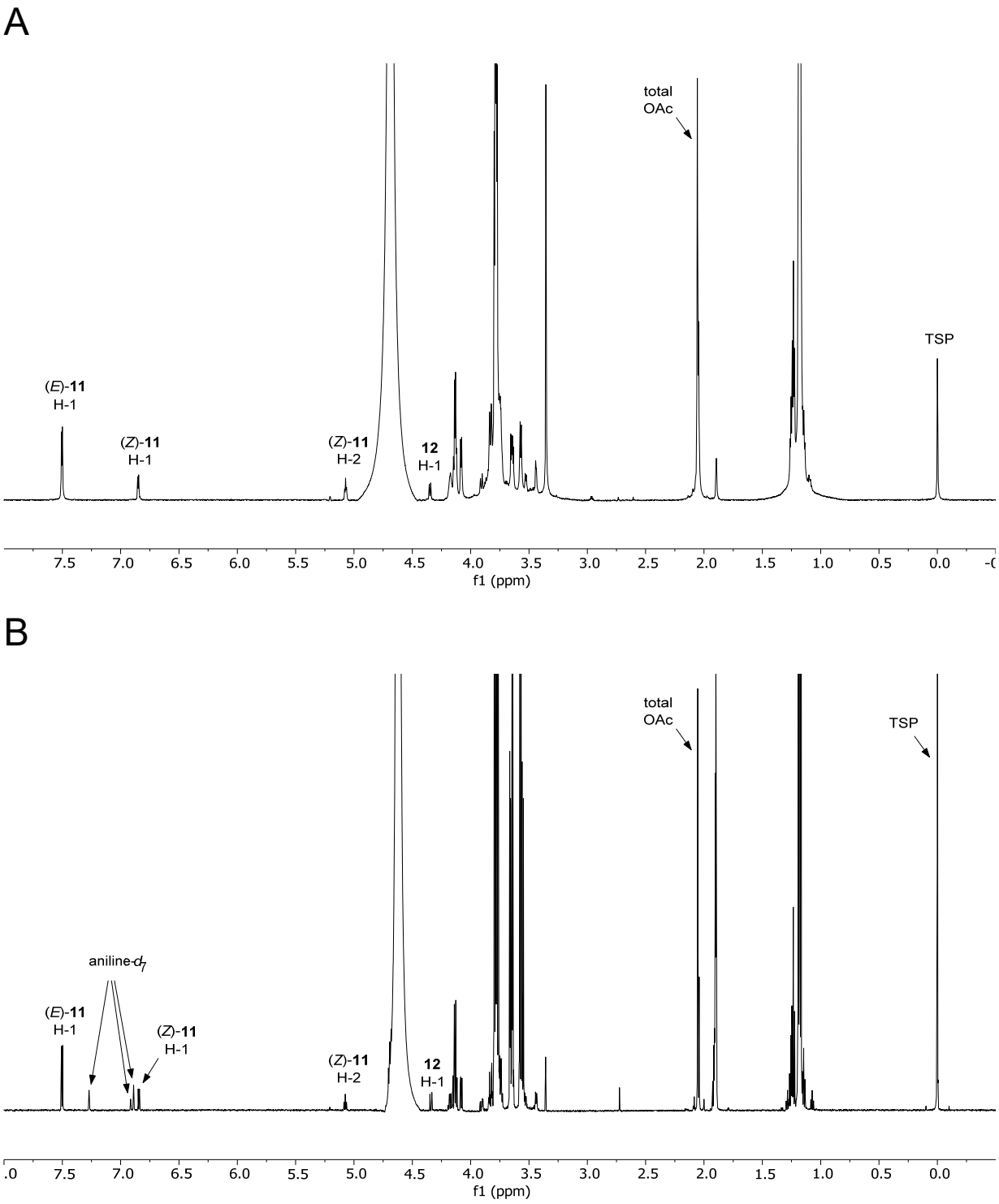

Figure S2. NMR spectra of the reaction mixtures of the reaction of (A) $GlcNAcNH_2$ **10** (36 mM) and ethoxyamine (180 mM) in 500 mM ammonium acetate-d_7 buffer at 39 °C and pH 6 after 10.3 h (800 MHz) and (B) GlcNAc (5 mM) and ethoxyamine (50 mM) with aniline-d_7 (100 mM) in 250 mM ammonium acetate-d_7 buffer at 39 °C and pH 6 after 400 h (600 MHz). Assignment of signals used for integration is shown. To be able to integrate signals close to the HDO peak at 4.6 ppm, multiple point baseline correction was carried out resulting in a peak form of the HDO peak deviating from a regular Lorentzian line.

Kinetic Treatment of Ligation Reaction

For a kinetic treatment of the amine ligation kinetics, the general reaction scheme (cf. Scheme 1) was reduced to the simplest form possible, comprising only the following three species (kinetic notation in parentheses): $GlcNAcNH_2$ **10** (**A**), GlcNAc (**B**) and reaction products (oximes and *N*-glycoside) (**P**) (Scheme S1).

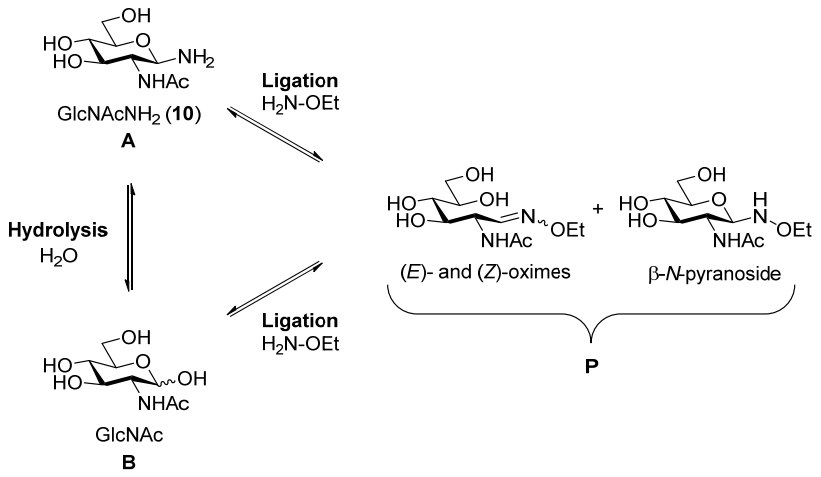

Scheme S1. Simplified reaction scheme for kinetic treatment.

The processes connecting these species were assumed to be of pseudo first order kinetics with pertinent first order rate constants as denoted in the following scheme:

$$\begin{aligned} \mathrm{A} &\underset{k_{-1}}{\overset{k_1}{\rightleftharpoons}} \mathrm{P} \\ \mathrm{A} &\underset{k_{-h}}{\overset{k_h}{\rightleftharpoons}} \mathrm{B} \\ \mathrm{B} &\underset{k_{-2}}{\overset{k_2}{\rightleftharpoons}} \mathrm{P} \end{aligned} \qquad \text{(S1a-c)}$$

Ligation of GlcNAc

Ligation of GlcNAc just represents the last reaction of the general scheme in equation (S1):

$$\mathrm{B} \underset{k_{-2}}{\overset{k_2}{\rightleftharpoons}} \mathrm{P} \qquad \text{(S1c)}$$

This is a simple equilibration kinetics and is described by the following time-dependence:

$$p(t) = \frac{k_2}{k_2 + k_{-2}}\left(1 - \exp[-(k_2 + k_{-2})t]\right) \qquad \text{(S2)}$$

The determination of k_2 and k_{-2} by exponential fitting is straight forward.

Ligation of GlcAcNH$_2$ 10

There are six rate constants in this case. It should be noted, however, that, for thermodynamic consistence, these cannot be chosen independently because the three chemical equations represent a cyclic reaction system **A** ⇄ **P** ⇄ **B** ⇄ **A** and the equilibrium constant for one half cycle: **A** ⇄ **P** ⇄ **B** must be equal to the equilibrium constant for the other half cycle: **B** ⇄ **A**. This requirement leads to the following equation for k_{-h}:

$$k_{\text{-h}} = k_{\text{h}} \frac{k_2 k_{-1}}{k_1 k_{-2}} \tag{S3}$$

The kinetic processes of eq. (S1) are represented by the following system of first order linear differential equations, wherein a, b and p denote the concentrations of the species **A**, **B** and **P**, respectively:

$$\dot{a}(t) = -k_1 a(t) - k_h a(t) + k_{-h} b(t) + k_{-1} p(t) \tag{S4a}$$

$$\dot{b}(t) = k_h a(t) - k_2 b(t) - k_{-h} b(t) + k_{-2} p(t) \tag{S4b}$$

$$\dot{p}(t) = k_1 a(t) + k_2 b(t) - k_{-1} p(t) - k_{-2} p(t) \tag{S4c}$$

The general solution of this system of linear differential equations can be represented as a sum of a constant and two exponential functions. If the rate constants of the two processes from **A** to **P** and from **B** to **P** are sufficiently different, a diagram of the product concentration versus a log(t) shows a double step function with a first plateau representing the product yield from **A** directly, while the hydrolysis product **B** is still unreacted. It is then followed by a step to a second plateau representing the total product yield. If k_1 is not significantly greater than k_2, an intermediate plateau will not be visible. In some cases, k_2 may be so small that the reaction seems to stop on the first plateau.

To solve the equations (S2) the software package Mathematica[5] was used. Finding the best fits of the rate constants was facilitated by using the graphical interactive Manipulate function. A working example is shown in Figure S3.

First guesses of the rate constants are taken in descending order of the size. In Figure S3a, the value of k_1 is set in such a way as to achieve best agreement in the beginning of the ascending part of the product curve. This leads to an overshooting in the later part and the plateau of the product curve. Adjusting the value of k_{h} (Figure S3b) can settle the second part of the rise of the product curve including its first plateau. There is a further increase of the product curve from the maximum to the final equilibrium value. Now, the value of k_2 is adjusted such that the time of the second inflection point of the product curve is met (Figure S3c). However, this leads to a further increase in the product yield. The final adjustment is done using $k_{\text{-1}}$ and $k_{\text{-2}}$. Their absolute values cannot be fixed unambiguously. To achieve the correct final level Y of the product yield, the two rate constants must fulfill the following linear correlation:

$$k_{-2} = k_2 \frac{1-Y}{Y} - \frac{k_2}{k_1} k_{-1} \tag{S4}$$

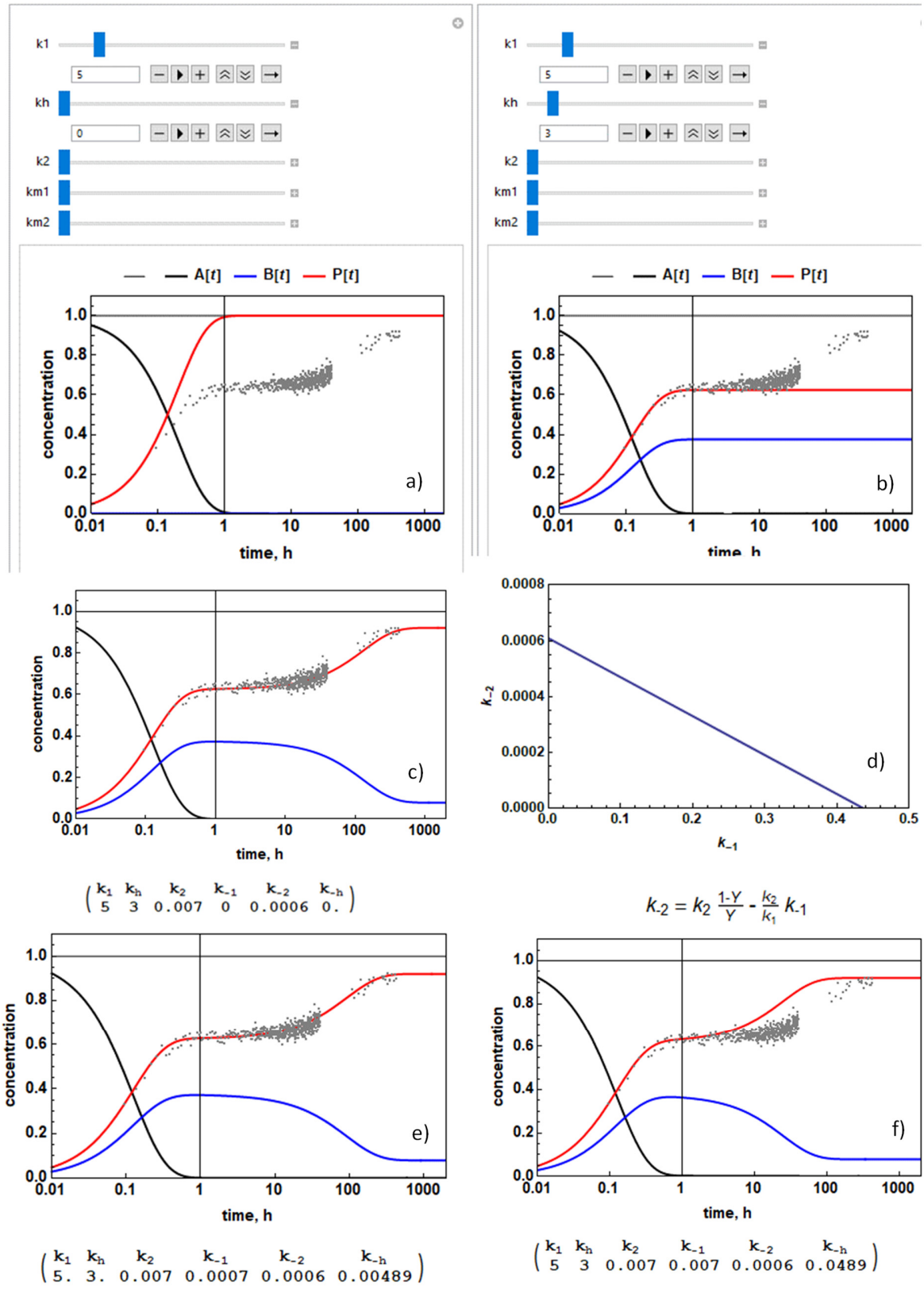

Figure S3. Stages of graphical determination of rate constants (case glycosyl amine in Fig. 3B) For explanation cf. text. Rate constants are given in units of h^{-1}.

Thus, one of them can be chosen rather freely. For the example given, the relation between k_{-2} and k_{-1} is shown as a diagram in Figure S3d. If k_{-1} is chosen close to zero, the rise kinetics to the second plateau remains determined by k_2. If, however, k_{-1} reaches the order of k_2, the second rise becomes faster (cf. Figure 2f). Thus, we fixed k_{-1} to about 1/10 of the value of k_2. The corresponding values of k_{-1} and k_{-2} are listed in Table S1 together with their boundaries defined by equation (S4).

Ligation of $GlcAcNH_2$ 10 – Extended Reaction System

In one case (cf. Figure 3A, reaction of glycosyl amine at pH 5), there is a third inflection point in the kinetic product curve. Such a behavior cannot be represented by a function with only two exponentials but needs a third exponential. The minimum requirement of the kinetic scheme is a fourth species **X**. This species must be produced from the ligation product P. Therefore, we extended the reaction scheme in two ways as indicated by Schemes S2A and S2B. In Scheme S2A, the additional species **X** is an intermediate on the way from **B** to **P**, which seems more realistically than inserting it between **A** and **P**, because the latter transformation is fast. In Scheme S2B, species **X** is produced from **P** but lies outside the reaction cycle constituted by the species **A**, **B**, and **P**.

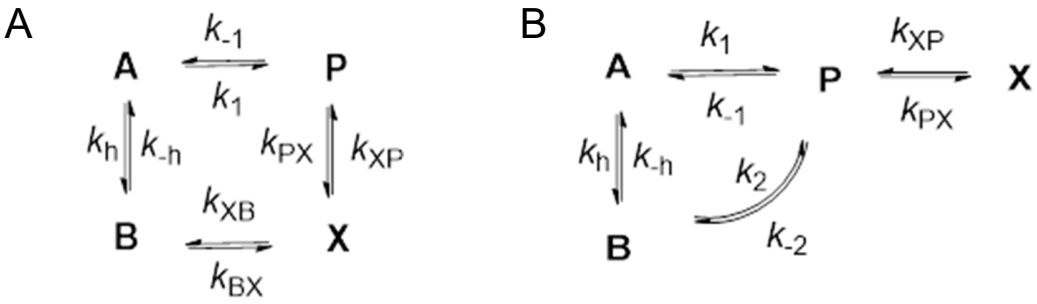

Scheme S2. Reaction schemes for kinetic treatment of the ligation reaction of $GlcAcNH_2$ **10** (**A**) according to Figure 3A. A) Additional species **X** between **A** and **P**, B) additional species **X** produced from **P** but outside the reaction cycle constituted by the species **A**, **B**, and **P**.

The two reaction schemes are described by the following systems of differential equations. In case of Scheme S2A we have

$$\dot{a}(t) = -k_1 a(t) - k_h a(t) + k_{-h} b(t) + k_{-1} p(t) \quad \text{(S5a)}$$

$$\dot{b}(t) = k_h a(t) - k_{-h} b(t) - k_{BX} b(t) + k_{XB} x(t) \quad \text{(S5b)}$$

$$\dot{x}(t) = k_{BX} b(t) - k_{XB} x(t) - k_{XP} x(t) + k_{PX} p(t) \quad \text{(S5c)}$$

$$\dot{p}(t) = k_1 a(t) - k_{-1} p(t) - k_{PX} p(t) + k_{XP} x(t) \quad \text{(S5d)}$$

In case of Scheme S2B we have

$$\dot{a}(t) = -k_1 a(t) - k_h a(t) + k_{-h} b(t) + k_{-1} p(t) \quad \text{(S6a)}$$

$$\dot{b}(t) = k_h a(t) - k_{-h} b(t) - k_2 b(t) + k_{-2} p(t) \quad \text{(S6b)}$$

$$\dot{x}(t) = k_{\mathrm{PX}} p(t) - k_{\mathrm{XP}} x(t) \quad \text{(S6c)}$$

$$\dot{p}(t) = k_1 a(t) + k_2 b(t) - k_{-1} p(t) - k_{-2} p(t) - k_{PX} p(t) + k_{\mathrm{XP}} x(t) \quad \text{(S6d)}$$

As stated above (cf. eq. S3), because of the reaction loop structure of both Scheme S2A and S2B, one of the rate parameters in the loop, for which we selected $k_{-\mathrm{h}}$, cannot be chosen independently. In case of Scheme S2B, eq. (S3) is still valid. In case of Scheme S2A, $k_{-\mathrm{h}}$ is given by:

$$k_{-\mathrm{h}} = k_{\mathrm{h}} \frac{k_{\mathrm{BX}}}{k_{\mathrm{XB}}} \frac{k_{\mathrm{XP}}}{k_{\mathrm{PX}}} \frac{k_{-1}}{k_1} \quad \text{(S8)}$$

The results of parameter fitting for reproducing the experimental kinetics according to Scheme S2A are shown in Figure S4, results based on Scheme S2B in Figure S5. In both cases, the intermediate minimum of the product concentration, when starting with species **A**, is reproduced. As represented in Figures S4a and S5a, in the first stage of the reaction, ending after about half an hour, product **P** is formed in competition with the hydrolysis product **B**. Next, formation of **X** from **P** occurs, a process accounting for a decrease of the concentration of **P**, which is made up again with a time constant of about 10 h, when **B** reacts to **P**, either directly (Scheme S2B) or via **X** (Scheme S2A). During the latter process the equilibrium between **P** and **X** is always maintained.

For each set of kinetic fitting parameters, we considered both alternatives of the reaction, either starting with species **A** or with species **B**. In the strict sense, the same set of kinetic parameters should fit the product formation kinetics, independent of the starting point. This requirement is closely fulfilled for Scheme S2B (Figure S5) but shows significant deviations for Scheme S2A (Figure S4), where the resulting kinetics for **P**, formed from **B**, (viz. **P**(**B**)) is shifted by a factor of about 1.5 to longer times than the observed data, if the parameters are optimized for the kinetics of **P**, formed from **A** (**P**(**A**), cf. Figure S4b)). On the other hand, the kinetics for **P** formed from **A** (**P**(**A**)) lies significantly below the observed data if the parameters are optimized for the kinetics of **P** formed from **B** (**P**(**B**), cf. Figure 4c). From such observations, one might conclude that Scheme S2B is the correct one. This conclusion is also supported when considering the possible structures of **X** for the two kinetic alternatives (cf. below).

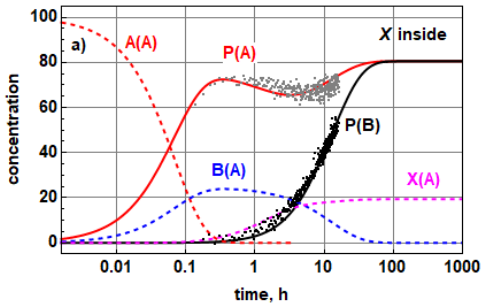

optimum compromise for parametrisation of product kinetics starting either with A or B

k_1	k_h	k_{BX}	k_{XP}	k_{-1}	k_{PX}	k_{XB}	k_{-h}
10.9	3.6	0.057	0.55	$7.\times10^{-5}$	0.13	0.0002	0.028

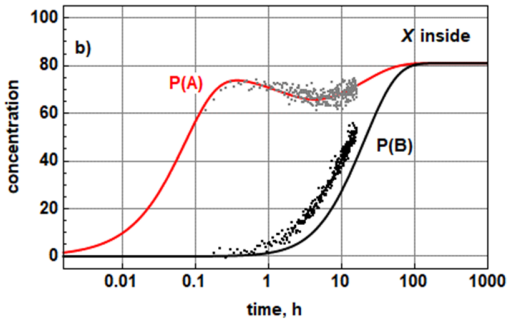

optimum for parametrisation of product kinetic when starting with A

k_1	k_h	k_{BX}	k_{XP}	k_{-1}	k_{PX}	k_{XB}	k_{-h}
10.4	3.2	0.04	0.47	5.4×10^{-5}	0.11	0.00026	0.011

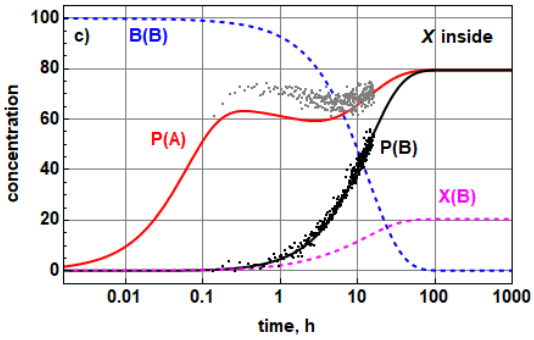

optimum for parametrisation of product kinetic when starting with B

k_1	k_h	k_{BX}	k_{XP}	k_{-1}	k_{PX}	k_{XB}	k_{-h}
10.4	5.5	0.025	0.42	$5.\times10^{-5}$	0.11	0.000035	0.072

Figure S4. Fit of the product formation kinetics according to Scheme S2A (species **X** "inside" the reaction cycle). a) Best compromise for fitting both alternatives, reactions starting either at **A** or **B**, with the same set of parameters. b) Best fit for reaction starting at **A**. c) Best fit for reaction starting at **B**. In a) the concentration profiles of **A**, **B**, and **X** are also shown, in c) the concentration profiles of **B** and **X** are also shown. In the symbols assigned to the kinetic curves, the symbol in brackets denotes the respective starting species.

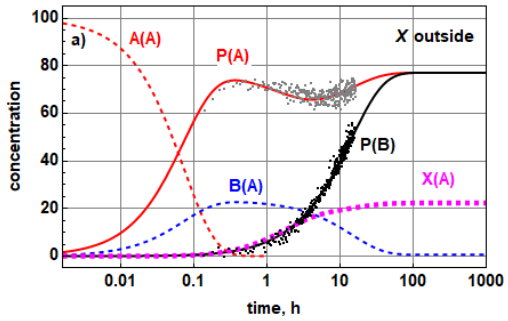

optimum compromise for parametrisation of product kinetics starting either with A or B

k_1	k_h	k_{PX}	k_{XP}	k_2	k_{-1}	k_{-2}	k_{-h}
10.6	3.2	0.13	0.46	0.051	0.0006	0.0004	0.023

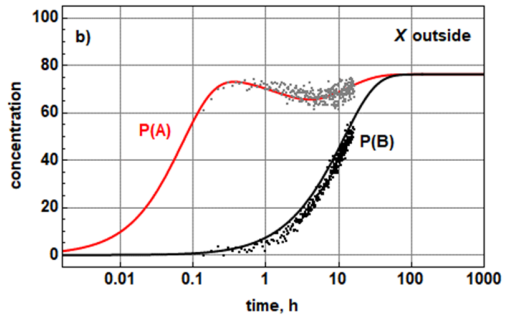

optimum for parametrisation of product kinetic when starting with A

k_1	k_h	k_{PX}	k_{XP}	k_2	k_{-1}	k_{-2}	k_{-h}
10.6	3.4	0.13	0.43	0.06	0.0006	0.00039	0.03

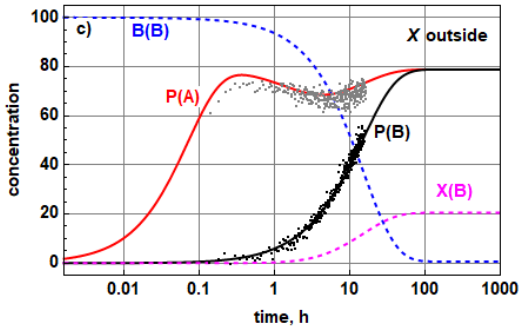

optimum for parametrisation of product kinetic when starting with B

k_1	k_h	k_{PX}	k_{XP}	k_2	k_{-1}	k_{-2}	k_{-h}
11.	2.9	0.12	0.47	0.05	0.0006	0.0004	0.02

Figure S5. Fit of the product formation kinetics according to Scheme S2B (species **X** "outside" the reaction cycle). a) Best compromise for fitting both alternatives, reactions starting either at **A** or **B**, with the same set of parameters. b) Best fit for reaction starting at **A**. c) Best fit for reaction starting at **B**. In a) the concentration profiles of **A**, **B**, and **X** are also shown, in c) the concentration profiles of **B** and **X** are also shown. In the symbols assigned to the kinetic curves, the symbol in brackets denotes the respective starting species.

Scheme S3 shows possible structures of product **X** according to the kinetic treatments shown in Scheme S2. In the case of product **X** being "inside" the reaction cycle constituted by the species **A**, **B**, and **P**, the hemiaminal formed by addition of ethoxyamine to the open-chain aldehyde form of GlcNAc is a possible candidate (Scheme S3A). However, in agreement with the literature,[6] the NMR spectra revealed no evidence of a hemiacetal species in equilibrium. In the case of product **X** being "outside" the reaction cycle constituted by the species **A**, **B**, and **P**, one may consider the aminal formed upon addition of a second ethoxyamine molecule to the (*E*)- or (*Z*)-oxime as a possible and more likely structure for **X** (Scheme S3B) which is also in agreement with the kinetic analysis above.

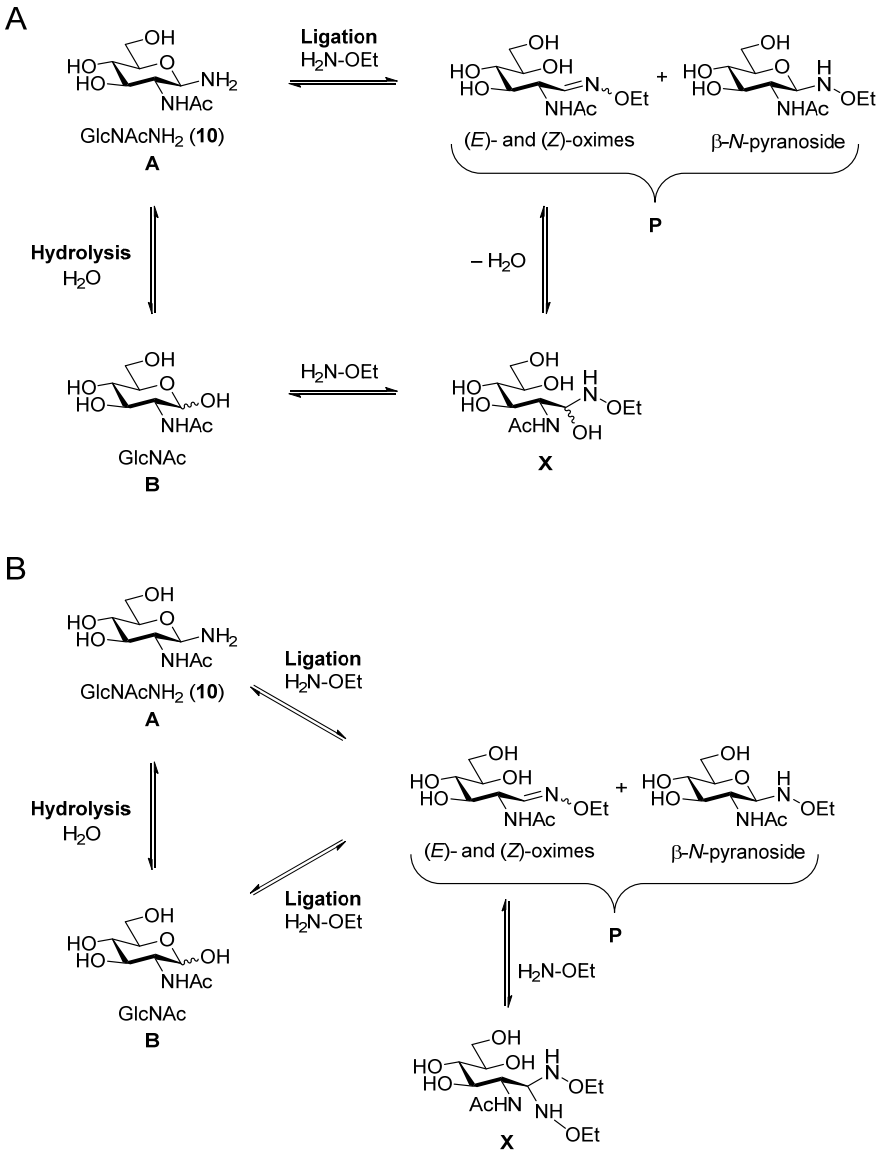

Scheme S3. Possible structures of product **X** according to the kinetic treatments shown in Scheme S2. A) Product **X** "inside" and B) product **X** "outside" the reaction cycle constituted by the species **A**, **B**, and **P**.

Table S1. Kinetic parameters of the fit curves shown in Figures 2 and 3. Kinetic constants are given in h^{-1}. An = aniline

	36 mM Sugar	pH	k1	k2	kh	k-1 (range)	k-2 (range)	k_{-h}	**Factor GlcNAcNH2 /GlcNAC**	**Factor GlcNAc+An /GlcNAC**
Fig. 2A	GlcNAcNH2	5	25	0,30	6,2	0,03 (0-3.8)	0.045 (0-0.045)	0,05	**83**	
Fig. 2A	GlcNAc+An	5	--	0,35	--	--	0,06	--		**1,2**
Fig. 2A	GlcNAc	5	--	0,3	--	--	0,027	--		
Fig. 2B	GlcNAcNH2	6	8	0,045	1,6	0,005 (0-0,44)	0,0045 (0-0,006)	0,0045	**160**	
Fig. 2B	GlcNAc+An	6	--	0,080	--	--	0,017	--		**1,6**
Fig. 2B	GlcNAc	6	--	0,050	--	--	0,012	--		
Fig. 2C	GlcNAcNH2	7	1,5	0,13	0,50	0,013 (0-0.6)	0,052 (0-0.055)	0,011	**150**	
Fig. 2C	GlcNAc+An	7	--	0,030	--	--	0,011	--		**3,0**
Fig. 2C	GlcNAc	7	--	0,010	--	--	0,004	--		
Fig. 2D	GlcNAcNH2	8	0,37	0,005	0,40	0,03 (0-0,15)	0,016 (0-0,02)	0,10	**74**	
Fig. 2D	GlcNAc+An	8	--	0,006	--	--	0,004	--		**1,2**
Fig. 2D	GlcNAc	8	--	0,005	--	--	0,003	--		

	5 mM Sugar	pH	k1	k2	kh	k-1	k-2	k_{-h}	**Faktor GlcNAcNH2 /GlcNAC**	
Fig. 3A	GlcNAcNH2[(1)]	5	10,6	0,06	3,4	0,0006	0,0004	0,03	**208**	
Fig. 3A	GlcNAc+An	5	--	0,25	--	--	0,035	--		**4,9**
Fig. 3A	GlcNAc	5	--	0,051	--	--	0,008	--		
Fig. 3B	GlcNAcNH2	6	5	0,007	3	0.0007 (0-0.043)	0.0006 (0-0.0006)	0,0049	**417**	
Fig. 3B	GlcNAc+An	6	--	0,040	--	--	0,006	--		**3,3**
Fig. 3B	GlcNAc	6	--	0,012	--	--	0,002	--		
Fig. 3C	GlcNAcNH2	7	0,55	0,015	0,30	0,001 (0-0,16)	0,0041 (0-0,0045)	0,003	**275**	
Fig. 3C	GlcNAc+An	7	--	0,010	--	--	0,003	--		**5,0**
Fig. 3C	GlcNAc	7	--	0,002	--	--	0,0006	--		
Fig. 3D	GlcNAcNH2	8	0,060	< 0,0007	0,06	--	--	--	**86**	
Fig. 3D	GlcNAc+An	8	--	0	--	--	0	--		**0,0**
Fig. 3D	GlcNAc	8	--	0,0007	--	--	0,001	--		
20 eq Ethoxyamine										
Fig. 3E	GlcNAcNH2	6	8,0	0,015	2,6	0,0015 (0-1.4)	0,002 (0-0.002)	0,0037	**500**	
Fig. 3E	GlcNAc+An	6	--	0,060	--	--	0,006	--		**3,8**
Fig. 3E	GlcNAc	6	--	0,016	--	--	0,003	--		
50 eq ethoxyamine										
Fig. 3F	GlcNAcNH2	6	12	0,02	1,5	0,002 (0-0,62)	0,001 (0-0.0011)	0,005	**200**	
Fig. 3F	GlcNAc+An	6	--	0,11	--	--	0,012	--		**1,8**
Fig. 3F	GlcNAc	6	--	0,06	--	--	0,004	--		

[1)] kinetics shows an intermediate minimum (dip) that is incompatible with the simple reaction scheme.
Data refer to fit with an extended kinetic model, involving a side-product X in equilibrium with P.

Kinetics of Hydrolysis

Most of the kinetics at pH 6 – 8 are not monoexponential, indicating that the process is not a one-step reaction. During the first 10 – 30% of hydrolysis, the kinetics is much fast than for the rest. Thus, except for the case of pH 5, biexponential fits were employed. The obtained fits and parameters are given in Figure S6.

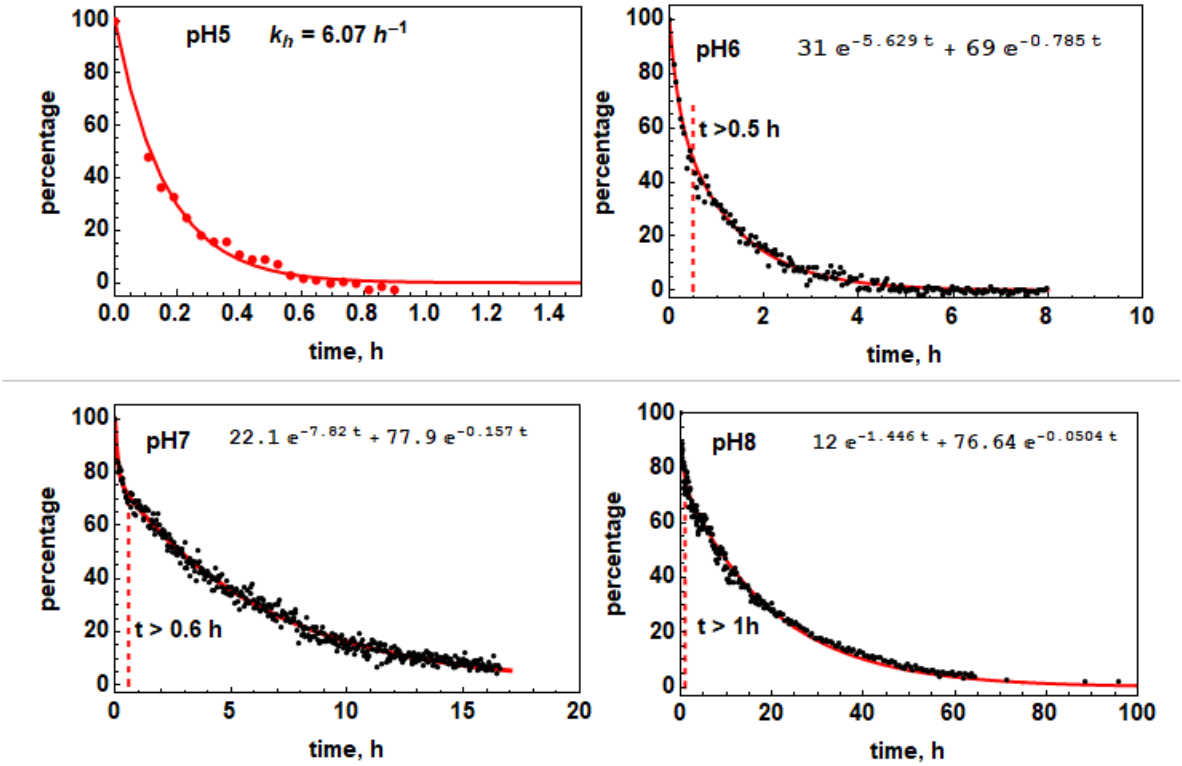

Figure S6. Data and fit curves for $GlcNAcNH_2$ hydrolysis at various pH values. Except for pH 5, the curve fits are biexponential. Beyond the given time limits, the curves decay monoexponentially with the smaller of the two exponential decay constants.

MS data of glycans released from RNase B and conjugated to linker 13

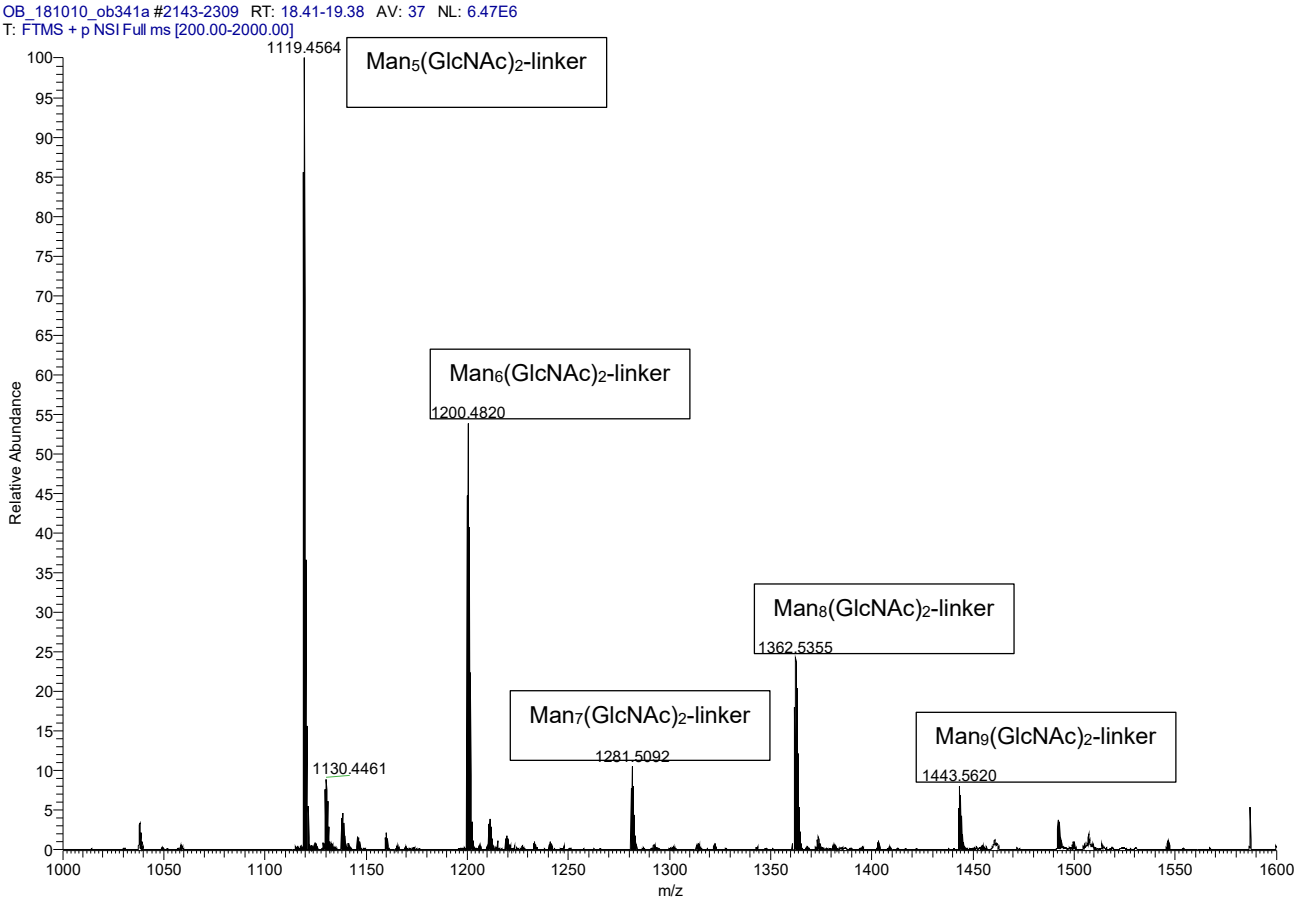

Figure S7. MS analysis of the mixture of glycans released from RNase B and conjugated to linker **13**.

References

1 T. Tanaka, H. Nagai, M. Noguchi, A. Kobayashi, S.-i. Shoda, *Chem. Commun.*, 2009, 3378-3379.
2 R. Joseph, F. B. Dyer, P. Garner, *Org. Lett.*, 2013, **15**, 732-735.
3 A. Krężel, W. Bal, *J. Inorg. Biochem.*, 2004, **98**, 161-166.
4 The synthesis of linker 13 was achieved in 8 steps starting from Fmoc-Lys(Boc)-OH and will be published elsewhere.
5 MATHEMATICA, *Version 11.2,*, 2017, Wolfram Research, Inc.: Champaign, Ill.
6 J. Kalia, R. T. Raines, *Angew. Chem., Int. Ed.*, 2008, **47**, 7523-7526.